Day-ahead Bidding Model for Virtual Power Plant Based on Segmented Bidirectional Pinch Forcing Theorem

Jianghong Nie*, Ling Gan and Nianbin Chen

*Corresponding author's e-mail: njh@hbepc.com, Second author's e-mail: 3640593490@qq.com, Third author's e-mail: NianbinChen@outlook.com

Hubei power exchange center, Wuhan, Hubei, 430048, China

Abstract. In developing the bidding strategy for the day-ahead market, the virtual power plant needs to forecast the marginal day-ahead market clearing tariff, as well as the output of wind turbines and photovoltaic (PV) units within the virtual power plant. The characteristic scenarios comprising the key risk factors can be classified by simultaneously considering the time-period levels of the key risk factors affecting the above three uncertain variables over the historical statistical period and by performing a cluster analysis of the curve similarity representations based on the segmented bi-directional pinch forcing theorem. By categorizing the results after predicting the values of the day-ahead key risk factors on a future date, i.e., the distribution of the three uncertain variables under the same category can be obtained, and the values of the uncertain variables can be predicted with a certain probability. The uncertain variables are brought into the objective function of virtual power plant bidding, the virtual power plant day-ahead bidding strategy can be obtained. The simulation results verify the effectiveness of the proposed method.

Keywords-virtual power plant; pinch forcing theorem; bidding model

1 Introduction

Virtual power plants, as entities with the ability to aggregate and manage distributed energy resources with efficient, flexible, and friendly grid-connection characteristics, are an important measure to deal with the problem of distributed energy access to the power syste m[1].Virtual power plants gain revenue by participating in the electric energy market and auxiliary service market. Virtual power plants gain revenue by participating in the electric energy market and auxiliary service market. Currently, virtual power plants participate in the market as price takers. Under this market mechanism, the decision of the virtual power plant to participate in the energy market is mainly based on the total amount of declarations and the allocation of generation within the virtual power plant through the estimated spot market price.

Current research on bidding for virtual power plants focuses on the formulation of objective functions, which are divided into two-tier/multi-stage bidding models and single-tier bidding models. The upper and lower objective functions of the two-tier/multi-stage bidding model are mostly related to maximizing the revenue of the virtual power plant, minimizing the cost of purchasing electricity, minimizing the total cost of purchasing energy in the market and

MSIEID 2023, December 08-10, Guangzhou, People's Republic of China

DOI 10.4108/eai.8-12-2023.2344465

minimizing the cost of scheduling, maximizing the total revenue of each market, minimizing the total cost of participation, maximizing the total profit, etc. [2-6]. Single-tier bidding models are mostly virtual power plant profit maximization, revenue maximization, etc [7]. Specific optimization methods used include master-slave game, Latin hypercube sampling method for generating scenarios, scenario reduction techniques, Monte Carlo, GAMS software and CPLEX solver, Copula function, particle swarm algorithm, stochastic planning methods, adaptive learning methods, robust optimization, artificial neural networks, etc [2-7]. The above methods involve some assumptions, such as the need to have or the ability to predict competitors' offer data when predicting spot market prices, the assumption that electricity price fluctuations are normally distributed, the assumption that various scenarios have equal probability of occurrence, and the assumption that the electricity price consists of the sum of the mean and random variables, which are more difficult to realize in the existing electricity market environment[8].

For the bidding strategy of virtual power plants participating in the day-ahead market as price takers, the model adopts a segmented bidirectional pinch forcing model to construct a curve similarity characterization between days and matrix clustering based on the characterization values. A day-ahead bidding model for virtual power plants based on the segmented bi-directional pinch forcing theorem is developed based on the similar day method for estimating the uncertain electricity price and new energy output.

2 Day-ahead bidding model for virtual power plants

2.1 Objective function

The profit maximization of the virtual power plant's participating in the day-ahead market is used as an objective function as follows

$$\max P_{\text{profit}} = R_{\text{revenue}} - C_{\text{cost}} \tag{1}$$

where, P_{profit} represents proceeds from the virtual power plant; R_{revenue} and C_{cost} are the revenues and costs of the virtual power plant, respectively.

2.1.1 Revenue components.

R_{revenue} include revenues from the virtual power plant's participation in the day-ahead market and revenues from the virtual power plant's sales of electricity to users:

$$R_{\text{revenue}} = \sum_{t=0}^{23} P_{lmp,t} \times Q_{t,\text{spot}} + \sum_{t=0}^{23} P_{dr,t} Q_{dr,t} \tag{2}$$

where, $P_{lmp,t}$ and $Q_{t,\text{spot}}$ are the day-ahead marginal market clearing tariff for time period t and the electricity sold by the virtual power plant for time period t, respectively; P_t and $P_{dr,t}$ are the pre-demand response tariff and the post-demand response tariff, respectively; $Q_{dr0,t}$ and $Q_{dr,t}$ are the original load and the responding load at time period t, respectively; $Q_{dr,t,pr}$ is the actual responding amount of user; ε is the coefficient of demand elasticity.

2.1.2 Cost components.

The total cost of the virtual power plant includes the cost of purchasing power in the day-ahead market, the cost of the gas-fired unit, and the degradation cost of the energy storage.

$$\begin{aligned} C_{\text{cost}} &= C_{\text{pe\_cost}} + C_{\text{gas\_cost}} + C_{\text{de\_cost}} \\ C_{\text{pe\_cost}} &= \sum_{t=0}^{23} P_{lmp,t} \times \left[Q_{dr,t} - Q_{t,\text{ wsf}} + P_{t,\text{ ch,e}} \times \Delta t - \eta_{dis} \times P_{t,\text{dis,e}} \times \Delta t \right] \\ C_{\text{gas\_cost}} &= \sum_{t=0}^{23} \sum_{n=1}^{N} \left[\left(\sum_{j=1}^{J} k_{n,j} P_{n,j,t,\text{out}} \right) + \varphi_{n,t,\text{start}} C_{n,\text{ start}} + \varphi_{n,t,\text{stop}} C_{n,\text{ stop}} \right] \\ C_{\text{de\_cost}} &= \sum_{t=T}^{T+L} \sum_{j=1}^{J} \Delta t \times C_j \times \left(\eta_{ch} P_{t,j}^{ch} + \frac{P_{t,j}^{dis}}{\eta_{dis}} \right) \end{aligned} \tag{3}$$

where, $C_{\text{pe\_cost}}$ is the cost of purchasing power in the day-ahead market; $C_{\text{gas\_cost}}$ and $C_{\text{de\_cost}}$ are the cost of the gas-fired unit and the degradation cost of the energy storage. $Q_{t,\text{ wsf}}$ is the total predicted wind and photovoltaic power generation in the virtual power plant at time period t ahead of the day. $P_{t,\text{ ch,e}}$ and $P_{t,\text{dis,e}}$ are the charging and discharging power of the energy storage devices in the virtual power plant at time period t, respectively; η_{dis} is is the discharge efficiency; $k_{n,j}$ is the slope of the generation cost of the n-th gas turbine at section j; $P_{n,j,t,\text{out}}$ is the output of the nth gas turbine at time period t in segment j. $\varphi_{n,t,\text{start}}$ and $\varphi_{n,t,\text{stop}}$ are binary variables for the start and stop of the n-th gas turbine at time period t, respectively; $C_{n,\text{ start}}$ and $C_{n,\text{ stop}}$ are start and stop costs for the n-th gas turbine, respectively; the value of the marginal aging cost C_j for the battery storage cycle depth segment j is tentatively set at \$0.009/(kWh).

2.2 Constraints on the objective function

The internal power balance constraints of the virtual power plant are shown below:

$$Q_{t,\text{w}} + Q_{t,\text{s}} + Q_{t,\text{gas}} + Q_{t,\text{dis}} = Q_{t,\text{sale}} + Q_{dr,t} + Q_{t,\text{ch}} \tag{4}$$

where, $Q_{t,\text{w}}$, $Q_{t,\text{s}}$, $Q_{t,\text{gas}}$ and $Q_{t,\text{dis}}$ are the generation of electricity from wind, photovoltaic, and gas units and the discharge of energy storage facilities in the virtual power plant at time period t,respectively; $Q_{t,\text{ch}}$ is the charging capacity of the energy storage facility in the virtual power plant for time period t.

The constraints for the gas unit are shown below:

$$
\begin{aligned}
&\varphi_{n,t,\text{work}} - \varphi_{n,t\text{-}1,\text{work}} \le \varphi_{n,t,\text{start}} \\
&\varphi_{n,t,\text{work}} - \varphi_{n,t\text{-}1,\text{work}} \le \varphi_{n,t,\text{stop}} \\
&P_n^{\min}\varphi_{n,t,\text{work}} \le P_{n,t} \le P_n^{\max}\varphi_{n,t,\text{work}} \\
&-r_n^d \le P_{n,t} - P_{n,t\text{-}1} \le r_n^u \\
&\sum_{t=1}^{t_n^{u}-t_n^{u,\text{initial}}} \left(1-\varphi_{n,t,\text{work}}\right) = 0 \\
&\sum_{t=1}^{t_n^{d}-t_n^{d,\text{initial}}} \varphi_{n,t,\text{work}} = 0 t_n^{u,\text{initial}}
\end{aligned}
\tag{5}
$$

where, $\varphi_{n,t,\text{work}}$ and $\varphi_{n,t\text{-}1,\text{work}}$ are binary variables for whether the nth gas turbine is working at time period t and time period t-1, respectively; $\varphi_{n,t,\text{start}}$ and $\varphi_{n,t,\text{stop}}$ are the binary variables for whether the n-th gas turbine starts and stops at time period t, respectively; $P_n^{\max}$ and $P_n^{\min}$ are the maximum and minimum output power of the n-th gas turbine, respectively; $P_{n,t}$ and $P_{n,t\text{-}1}$ are the output of the n-th gas turbine at time period t and time period t-1, respectively; r_n^u and r_n^d are the upward and downward ramping power of the n-th gas turbine, respectively; t_n^u and t_n^d are the minimum on and off times of the n-th gas turbine, respectively; $t_n^{u,\text{initial}}$ and $t_n^{d,\text{initial}}$ are the initial on and off times of the n-th gas turbine, respectively.

The constraints of the energy storage facility are shown below:

$$
\begin{aligned}
&0 \le P_{t,j}^{dis} \le P_{\max}^{dis} \\
&0 \le P_{t,j}^{ch} \le P_{\max}^{ch} \\
&I_t^{dis} + I_t^{ch} \le 1 \\
&e_{t,j} - e_{t-1,j} = \Delta t \times (P_{t,j}^{ch}\eta_{ch} - P_{t,j}^{dis} / \eta_{dis}) \\
&0 \le e_{t,j} \le \overline{e}_j \\
&E_{\min} \le \sum_{j=1}^{J} e_{t,j} \le E_{\max}
\end{aligned}
\tag{6}
$$

where, $P_{\max}^{dis}$ and $P_{\max}^{ch}$ are the maximum charging and discharging power of the battery storage, respectively; I_t^{dis} and I_t^{ch} are binary variables for discharge and charge, respectively; $e_{t,j}$ and $e_{t-1,j}$ are the energy stored by the energy storage in the cyclic depth segment j in time periods t and t-1, respectively; $\overline{e}_j$ is the charging capacity of the energy storage facility in the virtual power plant for time period t; $E_{\max}$ and $E_{\min}$ are the maximum charging and discharging power of the battery storage, respectively.

The wind/PV constraints are shown below:

$$
0 \le P_{t,\text{w/s}} \le P_{t,\text{w/s},\max} \tag{7}
$$

where, $\overline{e}_j$ is the output power of the wind/photovoltaic unit in time period t; $P_{t,\text{w/s},\max}$ is the maximum power generated by the wind/photovoltaic unit.

The demand response constraints are shown below:

$$\begin{aligned} &-Q_{dr,t}^{\max} \le Q_{dr,t,pr} \le Q_{dr,t}^{\max} \\ &-\Delta P_{dr} \le P_{dr,t} - P_t \le \Delta P_{dr} \end{aligned} \tag{8}$$

where, $Q_{dr,t}^{\max}$ is upper limit of transferable load for users; ΔP_{dr} is the upper limit on the amount of tariff change offered by the virtual power plant to demand response loads.

3 Model Uncertainty Variables Handling Based on Segmented Bidirectional Pinch Forcing Theorem

The electricity price and wind and PV unit output in the day-ahead market are uncertain variables. In this paper, we first select the key risk factors affecting the above three uncertain variables, combine the key risk factors as the labels of the day-ahead trading days there, and then use the segmented bidirectional pinch forcing theorem, combined with the matrix cluster analysis method, to cluster the labels, and the elements within the same cluster set are treated as similar days to each other, and it is assumed that as long as the labels of a day-ahead trading day in the future fall in a certain cluster set. The day-ahead market price of electricity and the output of wind power and photovoltaic units on this trading day are within the interval with the highest frequency of the distribution consisting of similar days under this cluster set.

3.1 Segmented bi-directional pinch forcing theorem and clustering

In this paper, temperature, primary energy price index, wind speed and solar intensity are selected as the key risk factors affecting the day-ahead market price of electricity and the output of wind and photovoltaic units, which are denoted by A, B, C and E, respectively. The historical statistical date is denoted by d (d=1,2,$\cdots$, D) and the 24 periods of each day-ahead trading day is denoted by t (t=0,1,2,$\cdots$, 23).

3.1.1 Segmented bi-directional pinch forcing theorem.

The curves for the key risk factors need to be normalized first.

In the case of key risk factor A, for example, the normalization of the d-day curve for the previous trading day is treated as follows:

$$\begin{aligned} L_{A,d,\min} &= \min\left\{L_{A,d,0,o}, \cdots L_{A,d,t,o}, \cdots L_{A,d,23,o}\right\} \\ L_{A,d,\max} &= \max\left\{L_{A,d,0,o}, \cdots L_{A,d,t,o}, \cdots L_{A,d,23,o}\right\} \\ L_{A,d,t} &= \frac{L_{A,d,t,o} - L_{A,d,\min}}{L_{A,d,\max} - L_{A,d,\min}} \end{aligned} \tag{9}$$

where, $L_{A,d,t,o}$ and $L_{A,d,t}$ are the temperature curves of d-day during the historical statistical period at time period t and the normalized temperature curves.

$$U_A = \{L_{A,1}, \cdots, L_{A,d}, \cdots L_{A,D}\}$$
$$U_{A,d} = \{L_{A,d,0}, \cdots L_{A,d,t}, \cdots L_{A,d,23}\} \tag{10}$$

U_A is the set of normalized temperature curves for the trading days before the statistical period; $L_{A,d}$ is the normalized temperature curve of the day before trading day d; $L_{A,d,t}$ is the normalized temperature curve of the day before trading day d at time period t.

After the curve normalization process, the base curve needs to be determined. Divide the simultaneous curves into a set, shown by $U_{A,d,t}$:

$$U_{A,d,t} = \{L_{A,1,t}, \cdots, L_{A,d,t}, \cdots L_{A,D,t}\} \tag{11}$$

Arbitrarily selecting a curve in the set U_A as a benchmark curve, and here selecting $L_{A,d}$, each of the 24 segments $L_{A,d,t}$ in $L_{A,d}$ is a benchmark curve for the same time period, i.e., the set of time-phased benchmark curves for which $L_{A,d}$ is selected as a benchmark curve is as follows:

$$U_{A,D} = \{L_{A,D,0}, \cdots, L_{A,D,t}, \cdots, L_{A,D,23}\} \tag{12}$$

Next, the segmented bidirectional pinch forcing model is constructed. Arbitrarily choosing a time period t to analyze the similarity of the curves for all the same time periods t in the statistical period within the set $U_{A,d,t}$ is achieved using a segmented bi-directional pinch forcing model, constructing the model objective function as follows:

$$\begin{aligned} &\min s_{A,D,t} \\ &s.t. \quad s_{A,D,t} = b_{A,D,t} - a_{A,D,t} \\ &\qquad b_{A,D,t} > a_{A,D,t} \\ &a_{A,D,t} L_{A,D,t} \le L_{A,d,t} \le b_{A,D,t} L_{A,D,t} \end{aligned} \tag{13}$$

where, $a_{A,D,t}$ and $b_{A,D,t}$ are the downshift and upshift coefficients of the curve, respectively; $a_{A,D,t} L_{A,D,t}$ and $b_{A,D,t} L_{A,D,t}$ are the curves that have the same shape as the curve $L_{A,D,t}$ in segment t of the base price curve and lie below and above, respectively; $s_{A,D,t}$ is the value that characterizes the similarity between the curves, the smaller it is, the closer $a_{A,D,t}$ and $b_{A,D,t}$ are, the closer $a_{A,D,t} L_{A,D,t}$ and $b_{A,D,t} L_{A,D,t}$ are to the base curve $L_{A,D,t}$, and when it is 0 the objective function is optimal, i.e., it is completely overlapped.

By constructing a segmented bidirectional pinch model for all time periods, a set of curves with similarity $S_A = \{S_{A,0}, \cdots S_{A,t}, \cdots S_{A,T}\}$ can be obtained:

$$\begin{aligned} &S_{A,0} = \{s_{A,1,0}, \cdots, s_{A,d,0}, \cdots s_{A,D,0}\} \\ &\cdots \\ &S_{A,t} = \{s_{A,1,t}, \cdots, s_{A,d,t}, \cdots s_{A,D,t}\} \\ &\cdots \\ &S_{A,T} = \{s_{A,1,T}, \cdots, s_{A,d,T}, \cdots s_{A,D,T}\} \end{aligned} \tag{14}$$

The segmented two-way pinch forcing model is constructed for all time periods to obtain the set of simultaneous curve similarity， $R_A = \left\{ R_{A,1}, \cdots R_{A,d}, \cdots R_{A,D} \right\}$

$$\begin{aligned} & R_{A,1} = \left\{ s_{A,1,0}, \cdots s_{A,1,t}, \cdots s_{A,1,T} \right\} \\ & \cdots \\ & R_{A,d} = \left\{ s_{A,d,0}, \cdots s_{A,d,t}, \cdots s_{A,d,T} \right\} \\ & \cdots \\ & R_{A,D} = \left\{ s_{A,D,0}, \cdots s_{A,D,t}, \cdots s_{A,D,T} \right\} \end{aligned} \tag{15}$$

Similarly, the set of curve similarities, S_B, S_C, S_E, R_B, R_C, R_E, can be obtained for the other key risk factors B, C, and E.

3.1.2 Cluster analysis of matrices.

Based on the previous steps the 4-dimensional key risk factor segmented curve similarity characterization matrix for D days (i.e., D samples) can be obtained, and in the case of day d, the curve matrix S_d for day d is:

$$\begin{bmatrix} s_{A,d,0} & s_{A,d,1} & \cdots & s_{A,d,t} & \cdots & s_{A,d,23} \\ s_{B,d,0} & s_{B,d,1} & \cdots & s_{B,d,t} & \cdots & s_{B,d,23} \\ s_{C,d,0} & s_{C,d,1} & \cdots & s_{C,d,t} & \cdots & s_{C,d,23} \\ s_{E,d,0} & s_{E,d,1} & \cdots & s_{E,d,t} & \cdots & s_{E,d,23} \end{bmatrix} \tag{16}$$

Therefore, the D samples were subjected to a cluster analysis of the matrix to classify the similarity curves considering the four dimensions into one group. The samples were clustered using K-means clustering algorithm [11].

3.2 Uncertain variable prediction based on similarity days

3.2.1 Predicting segment values for key risk factors.

Assuming that the segmented key risk factor values for a day in a given year are similar to the segmented risk factor values for the same day in a calendar year, the composite weighted average of the segmented key risk factor values for the same day in a calendar year can be used to estimate the risk factor values for future segments for the same day. Therefore, the following model is used to predict the segmented key risk factor values for a future date:

$$\begin{aligned} & D_{\mathrm{f},A,t} = \left[\sum_{i=1}^{n} x_{i,A,t} \times k_i \right] \times \frac{x_{A,m-1,t}}{x_{A,1,m-1,t}} \\ & \sum_{i=1}^{n} k_i = 1 \end{aligned} \tag{17}$$

where $D_{\mathrm{f},A,t}$ is the value of the temperature in the time period of the forecast day; $x_{i,A,t}$ is the value of the temperature in the time period of the same day in the i-th year and forecast day of the statistical period t; k_i is the weight of the i-th year of the statistical period (n years

in total); $a_{A,t}$ is the percentage of the adjustment of the temperature in the recent past; $x_{A,m-1,t}$ is the value of the risk factor of the temperature in the time period of the day of the recent adjustment; $x_{A,1,m-1,t}$ is the value of the risk factor of the temperature in the time period of the same day in the year prior to the day of the recent adjustment. The adjustment factor $a_{A,t}$ is added here to take into account the overall variation between years in the prediction of the risk factor values.

Similarly, the segmented values of the other key risk factors $D_{\mathrm{f},B,t}$, $D_{\mathrm{f},C,t}$ and $D_{\mathrm{f},C,t}$, for a future date can be obtained. after section 3.1 the set of curve similarities, $S_{\mathrm{f},A}$, $S_{\mathrm{f},B}$, $S_{\mathrm{f},C}$, $S_{\mathrm{f},E}$, $R_{\mathrm{f},A}$, $R_{\mathrm{f},B}$, $R_{\mathrm{f},C}$, $R_{\mathrm{f},E}$, can be obtained for the prediction date, and also the curve matrix S_{f} for the prediction date can be obtained:

$$\begin{bmatrix} s_{A,\mathrm{f},0} & s_{A,\mathrm{f},1} & \cdots & s_{A,\mathrm{f},t} & \cdots & s_{A,\mathrm{f},23} \\ s_{B,\mathrm{f},0} & s_{B,\mathrm{f},1} & \cdots & s_{B,\mathrm{f},t} & \cdots & s_{B,\mathrm{f},23} \\ s_{C,\mathrm{f},0} & s_{C,\mathrm{f},1} & \cdots & s_{C,\mathrm{f},t} & \cdots & s_{C,\mathrm{f},23} \\ s_{E,\mathrm{f},0} & s_{E,\mathrm{f},1} & \cdots & s_{E,\mathrm{f},t} & \cdots & s_{E,\mathrm{f},23} \end{bmatrix} \tag{18}$$

The resulting curve matrix is categorized into the matrix classification results obtained in 3.1.2.

3.2.2 Prediction of Uncertain Variables and Day Ahead Bidding Decision Making.

A histogram of the frequency distribution of electricity price, wind power output, and PV output for all sample days in the classification where the curve matrix is located is composed. By identifying the highest interval of frequency, the value of uncertain variables on the forecast day can be predicted. The prediction results of uncertain variables are substituted into the virtual power plant day-ahead bidding model to develop day-ahead bidding decisions.

4 Simulation analysis

A virtual power plant containing gas-fired units, energy storage facilities, wind power, photovoltaic, and demand response loads is used as an example for arithmetic analysis. The parameters of the gas unit are adopted from Appendix A of literature [3]; the parameters of the energy storage facility are adopted from literature [9]; and the demand response tariff is designed according to the conclusion of literature [10], i.e., the peak-to-valley difference is $0.5/kWh. The demand response elasticity coefficient is designed using the parameters of literature [11].

4.1 Predicted results for uncertain variables

For simplicity of calculation, the 24 time periods were divided into peak, flat and valley periods, and the temperature, primary energy price, wind speed and sunlight intensity were selected as samples for the whole year of a certain year. Among them, the temperature, wind speed and sunlight intensity are selected as the temperature, wind speed and sunlight intensity

of a certain year in province G (using the amount of solar radiation reaching the horizontal surface of the earth's surface minus the amount reflected from the earth's surface). Primary energy prices are selected from the power coal prices in the same year and simulated in the dataset (more data need to be simulated because the power coal prices are published on a weekly basis and are processed in a randomized manner ± 0.5% on the basis of the source data). And statistics on the weighted average marginal clearing price of electricity in the peak and trough segments of the market before the day of the virtual power plant in this year, the turbine output within the virtual power plant and the PV unit output. The source data of temperature, primary energy price, wind speed, and light intensity are data processed and similarity matrices are obtained using equations (9) to (15) with a matrix size of 1098 × 4.

Cluster analysis of three times four-dimensional key risk factor portfolio similarity matrices were performed separately, and this example uses K-means clustering algorithm with Euclidean distance squared for clustering and the number of clusters was categorized into 3 classes. The temperature, primary energy price, wind speed, and light intensity for the predicted daily peak, flat, and valley hours are -3.43°C, $493.50/ton, 2.26 m/s, and 8,818,985 MJ/m2; -5.05°C, $497.25/ton, 1.53 m/s, and 8,707,584 MJ/m2; and -6.58°C, $494.82/ton, 1.70 m/s, and 0 MJ/m2, respectively. s, 0 MJ/m2. After the data processing of Eqs. (9) to (15), the categorization was performed using Matlab. According to the classification results, the intervals with the highest frequency in the distribution of tariffs, wind turbine output, and photovoltaic turbine output for the second category of the peak section, the first category of the flat section, and the second category of the valley section are identified, respectively, which are automatically realized using Matlab's histogram function. Take the peak section as an example, as shown in the figure 1. In addition, the highest frequency intervals corresponding to the electricity price, wind turbine output, and PV unit output for the first category of the flat section and the second category of the valley section are [360,390], [10,20], [6,8], [300,330], [0,20], and [0,0], respectively. Thus taking the midpoint of the interval gives the predicted levels of tariffs, wind turbine output, and PV unit output during peak, flat, and valley hours as [405,10,37.5], [375,15,7], and [315,10,0], respectively.

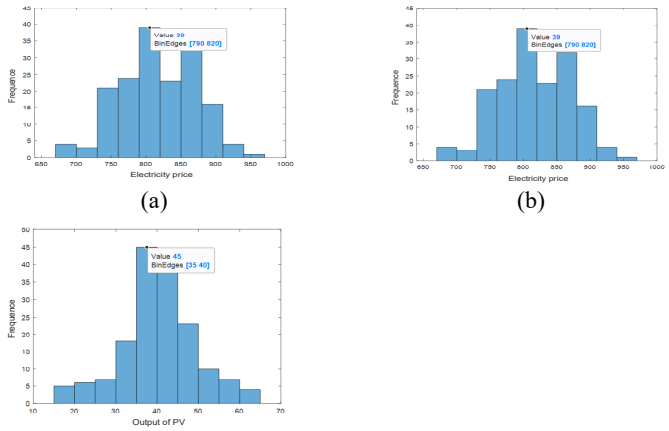

Figure 1. Distribution of electricity price, wind power output, and PV output under the second type of curve in the peak period.

4.2 Bidding decision making

As an example, the bidding decision making for the peak period is formulated using Matlab software by defining the objective function and constraints and outputting a feasible domain as shown in Fig. 2. Among them, each dimension represents: the amount of peak-segment bids in the market before the virtual power plant day, the peak-segment customer demand response tariff formulated by the virtual power plant, the load after the customer demand response, the power of energy storage charging/discharging in the peak-segment, and the output level of the gas unit. Where the x-axis, y-axis and z-axis represent the three axes in the five-dimensional space, respectively, with colors distinguishing the values of the other dimensions.

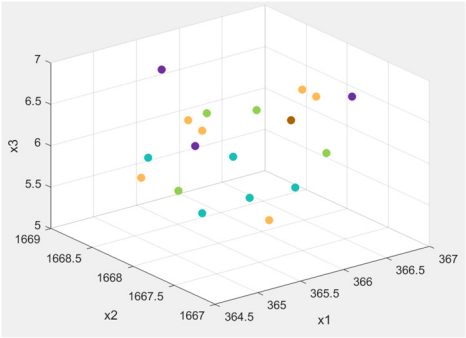

Figure 2. Feasible domain of the objective function.

The optimal solution is: the bidding output of the virtual power plant during peak hours is 265.7MWh, the user demand response electricity price set by the virtual power plant during peak hours is 1418 yuan/MWh, the load after user demand response is 4.2MW, the power discharged during peak hours is 10MW, and the output of the gas turbine is 5.7MW. The profit of the virtual power plant is 28685 yuan. The actual profit of the virtual power plant is within a deviation of 9% of the simulated profit, and the model is effective.

5 Conclusion

In this study, based on the segmental pinch forcing theorem and cluster analysis, we set up a method to predict the uncertain variables affecting the bidding strategy of the virtual power plant, and construct the objective function and constraints model of the virtual power plant, and finally derive the feasible domain of the prediction results, and obtain the bidding strategy to maximize the profit of the virtual power plant through the software. The use of multi-dimensional data and data normalization, similar multi-dimensional data matrix clustered into one class, helps the virtual power plant in the decision-making in the consideration of the distribution of electricity prices, wind power output, photovoltaic output in a similar market environment, the data is not simulated by the normal distribution, with authenticity and reliability, closer to the market real clearing situation. The virtual power plant can achieve the purpose of rationally adjusting the bidding strategy according to the day-ahead marginal clearing tariff by setting the internal demand response tariffs and allocating the output situation of gas units and energy storage facilities.Positioning tables.

Acknowledgments. This work was financially supported by the Research on Optimization Strategy of Hubei Electricity Spot Market Settlement Mechanism in 2023 (ZHNY2023-11).

References

[1] Naval N, Sánchez R., Yusta J. M. (2020). A virtual power plant optimal dispatch model with large and small-scale distributed renewable generation. Renewable Energy. 151, 57-69.
[2] Naval N, Yusta J. M. (2021). Virtual power plant models and electricity markets-A review. Renewable and Sustainable Energy Reviews. 149, 111393.
[3] ZHOU Y.Z, SUN G.Q, HUANG W.J, et al. (2017) Strategic Bidding Model for Virtual Power Plant in Different Electricity Markets Considering Electric Vehicles and Demand Response. Power System Technology. 41(06):1759-1767.
[4] SONG W, WANG J.W, ZHAO H.B, et al. (2017) Research on multi-stage bidding strategy of virtual power plant considering demand response market. Power System Protection and Control. 45(19):11
[5] ZHOU R.J, LV J, ZHANG WJ, et al. (2018) Bidding Strategies for Gas-Electricity Virtual Power Plants in Multi-energy Market. Electric power. 51(07):120-127.
[6] HE Q.L, AI Q, (2019)Bidding Strategy of Electricity Market Including Virtual Power Plant Considering Demand Response Under Retail Power Market Deregulation. Electric Power Construction. 40(02):1-10.
[7] Foroughi M., Pasban A., Moeini-Aghtaie M., et al. (2021). A bi-level model for optimal bidding of a multi-carrier technical virtual power plant in energy markets. International Journal of Electrical Power & Energy Systems. 125, 106397.
[8] ZHAO S.Q, YAO J.M, LI Z.W, (2021) Wind Power Scenario Reduction Based on Improved K-means Clustering and SBR Algorithm. Power System Technology. 45(10):3947-3954.
[9] LIU Q.X, LIU M.B, LU W.T, (2021)Control Method for Battery Energy Storage Participating in Frequency Regulation Market Considering Degradation Cost. Power System Technology. 45(08):3043-3051.
[10] SUN Y.J, WANG Y, WANG B.B, et al. (2018) Multi-time Scale Decision Method for Source-Load Interaction Considering Demand Response Uncertainty. Automation of Electric Power Systems. 42(02):106-113+159.
[11] KONG X.Y, YANG Q, MU Y.F, et al. Analysis Method for Customers Demand Response in Time of Using Price. Proceedings of the CSU-EPSA. 27(10):75-80.